

Muhammad Atif<sup>1</sup>, XianZhe Shi<sup>1</sup>, Muhammad Amir Raza<sup>1</sup>, Muhammad Zakir Sheikh<sup>1</sup>  
Jianghua Shen<sup>1,2</sup>, Yulong Li<sup>2,3,4</sup>

<sup>1</sup> School of Aeronautics and Institute of Extreme Mechanics, Northwestern Polytechnical University, Xi'an, 710072, Shaanxi, PR China.

<sup>2</sup> Joint International Research Center of Impact Dynamics and Its Engineering Application

<sup>3</sup> Shaanxi Key Laboratory of Impact Dynamics and its Engineering Applications, Xi'an, Shaanxi, China 710072

<sup>4</sup> School of Civil Aviation, Northwestern Polytechnical University, Xi'an, Shaanxi, China 710072

### Abstract

The modern transportation sector, including aerospace and defense, demand advanced materials with extraordinary properties to make the service structures more durable and safer. The aforesaid applications involve high-velocity impact and strain rate situations, in which structures may be subjected to radically different loading circumstances than their static equivalents. A new era of materials, namely multicomponent alloys that deviate from the conventional alloying strategy, is expected to replace traditional materials in future engineering applications. The reasons for this specific and notable commitment are their exceptional mechanical performance at room, high, and cryogenic temperatures. These alloys provide a consortium of properties that can outclass many materials currently in use. Such an alloy, namely Cantor alloy, an equiatomic, five-element material system CoNiFeMnCr has been tested under low and high strain rates. A remarkable elevated yield strength of 70% as compared to static loading, with high strain rate sensitivity and work hardening, is observed without fracture. This alloy's outstanding impact resistance makes it a prime contender for shock absorption and damage tolerant applications. The higher strength contribution at dynamic testing is linked to the profound effect of dislocation-mediated microstructural manifestation. The study also provides insights into a novel high strain rate method to evaluate impact-related problems in a precise, more versatile manner.

**Keywords:** High entropy alloy, strain rate sensitivity, ESHPB, work hardening

## **1. Introduction**

Unlike the conventional alloys based on iron, copper, or aluminum, high entropy alloys are materials that deviate from the traditional alloying strategy and are composed of at least five elements blended in a nearly equiatomic ratio. This manifestation attributes properties that are far better than conventional materials. Interestingly, superior mechanical properties are governed by phase adjustments like dual-phase alloys or by the severe plastic deformation methods. However, the high entropy alloys, in most scenarios, are stable single-phase alloys. However, their mechanical performance is far better than many conventional single-phase and dual-phase alloys. The development idea was floated in 2004 [1, 2], and it was investigated that four core effects, namely high entropy, sluggish diffusion, cocktail, and lattice distortion, contribute to the remarkable physical and mechanical properties of these materials. Amongst these effects, lattice distortion and cocktail are primarily concerned with the mechanical performance of alloys due to the atomic level strains and composite type effect governed by the equimolar nature of the elements present [3]. Another prominent and amongst the most influential attribute of high entropy alloys is the stacking fault energy which plays a controlling role in many deformation processes. Mostly the SFE of high entropy alloys is much lower as compared to conventional materials; for example, copper has SFE in the range of 78 mJ/m<sup>2</sup> whereas much high entropy and medium entropy alloys have SFE in the range of 15-30 mJ/m<sup>2</sup>. The lower SFE favors additional deformation mechanisms such as twinning in metals.

The Cantor alloy, consisting of five elements Co, Cr, Ni, Mn, and Fe, has been researched extensively and shows excellent mechanical properties, including high strength and ductility with a moderate yield strength at quasi-conditions of loading. A prominent manifestation of this alloy is its outstanding impact and shock resistance at high strain rates, as reported [4]. This elevated level of strengthening at a dynamic regime is governed by lattice defects and deformation mechanisms that initiate and are followed during the progression of straining under impact loading.

The deformation mechanisms are broadly categorized into dislocation mediated [5, 6] and or coupled with other interface defects like twins [6] in materials where the microstructure is strain rate sensitive. Keeping in view the complex and unique nature of these alloys, the recent regime of scientific research has witnessed a swift pace in the investigation of these alloys regarding various aspects ranging from microstructure [7] processing [8-10] and mechanical characterization [11, 12]. Fewer studies have been conducted to evaluate the dynamic performance of high entropy alloys [13, 14], yet a deep understanding of the phenomenological mechanisms is scarce.

Structural integrity for materials working under extreme conditions of load, impact, and crashworthiness is of prime concern in the transportation industry, specifically aerospace and defense, that demands extended safety of structural components. All these extreme conditions encounter service conditions that are entirely diverse compared with quasi-static loadings or static impacts. The borderline defining these scenarios of loading is the duration of impact; for example, at high strain rates, materials encounter high-temperature rise, and the dissipation of heat from the material is not possible, which in turn can cause softening effect and loss of strength making the structures vulnerable to damage.

Considering the vital field of impact and shock loading in aerospace and defense, the current study investigates the five-component based high entropy alloy, CoNiFeMnCr, at different strain rate regimes using a novel electro-magnetic split Hopkinson pressure bar proposed and developed by Li et al. [15, 16]. The study shows that the material under investigation bears a unique combination of strength and deformability, which is not affected by the high strain rate; rather, at the diverse loading conditions, the material provides high damage tolerance. The results will be helpful to broaden and pave the futuristic applications of this new class of materials in aforesaid industries.

## **2. Materials and methods**

High entropy alloy consisting of five elements, namely CoNiFeMnCr, was produced by a magnetic levitation furnace under vacuum conditions. The powders with elemental purity of more than 99.95 %

were used as raw material to produce the cast rods. The melt homogeneity was achieved by successive remelting of the cast ingot. Also, the material after casting was homogenized at a low-temperature range of 600°C for 6 hours in a vacuum to eliminate the effect of elemental segregation, if any. The chemical composition and phase identification was carried out by disruptive energy Spectroscopy (EDS) and X-ray diffraction (XRD), respectively. The microstructural characterization for the raw material and the deformed specimens was furnished using a Scanning electron microscope, Sigma-300, equipped with EBSD. The samples for EBSD were prepared using conventional grinding (800-2000 grit) followed by electropolishing employing HClO<sub>4</sub>: C<sub>2</sub>H<sub>2</sub>OH (1:9) at 20 V. Compression tests were carried out under quasi-static loading utilizing a servo-hydraulic universal testing machine while dynamic tests were conducted using indigenously developed ESHPB which uses electrical energy to acquire mechanical impact as compared to conventional split Hopkinson bar where pneumatic pressure is utilized to impact the striker. In the ESHPB, no striker bar is used, and only incident and transmitted bars are used as means of achieving high energy impact. A schematic of the ESHPB is shown in Figure 1. The capacitance plays a role in achieving the impact pulse duration, whereas the amplitude of the wave is controlled by voltage. The simple and constant combination of capacitance and voltage makes it possible to achieve the precise and well-controlled impact energy as compared to conventional SHPB, where pressure variations and mismatch between striker and incident bar usually result in varying pulse amplitude and hence the strain rate.

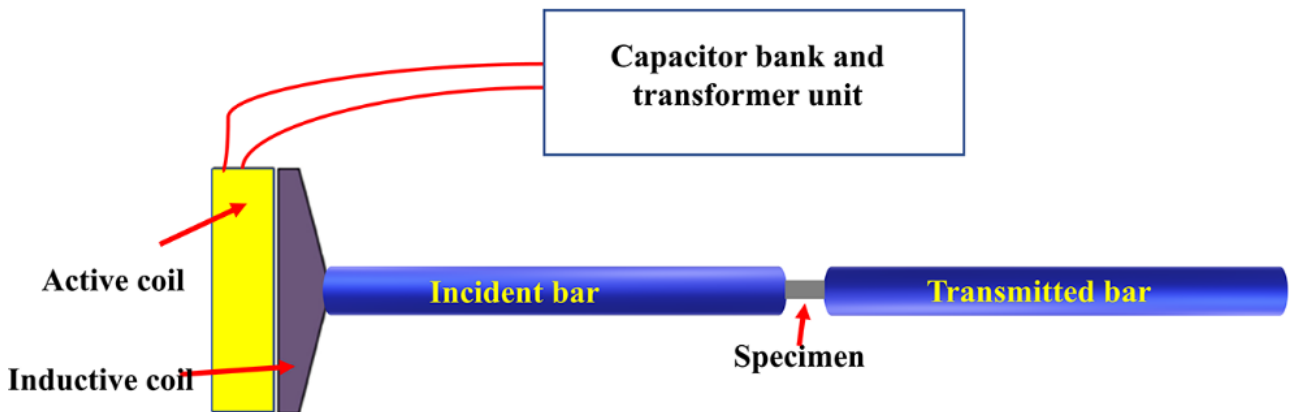


Figure 1: Schematic of electro-magnetic split Hopkinson bar

Square-shaped specimens with dimensions of 4x4x4 mm<sup>3</sup> were prepared by electric discharge cutting. For comparison purposes, conventional FCC material, copper, was also tested under the same loading conditions. Before tests, the specimens were mechanically polished to remove the surface roughness and make the contact-surface parallel to avoid any stress concentration.

### 3. Results and discussion

#### 3.1 Pre-compression microstructural characterization

XRD was used to characterize the high entropy alloy for phase identification. The scanning speed for XRD was chosen as 3 °/ min, and the scanning angle was swept between 30 to 120 °. The phase map is shown in **Figure 2** (a), profiling well-defined XRD peaks corresponding to single-phase FCC alloy. Also, the homogeneous and equimolar nature is clearly evident from the EDS maps and chemical composition displayed in **Figure 2** (b), respectively. Some black spots are observed in the individual EDS maps, which correspond to porosity in the material. Being a cast product, porosity is inherent to materials; however, the distribution of alloying elements is homogeneous (as verified by EDS), which is a pre-requisite in all the high entropy alloys along with single or multiple phase formations and their stability. After the compression testing, samples were microscopically examined, and the results are presented in **Figure 5**. Details regarding salient features of the corresponding microstructural evolution are discussed later.

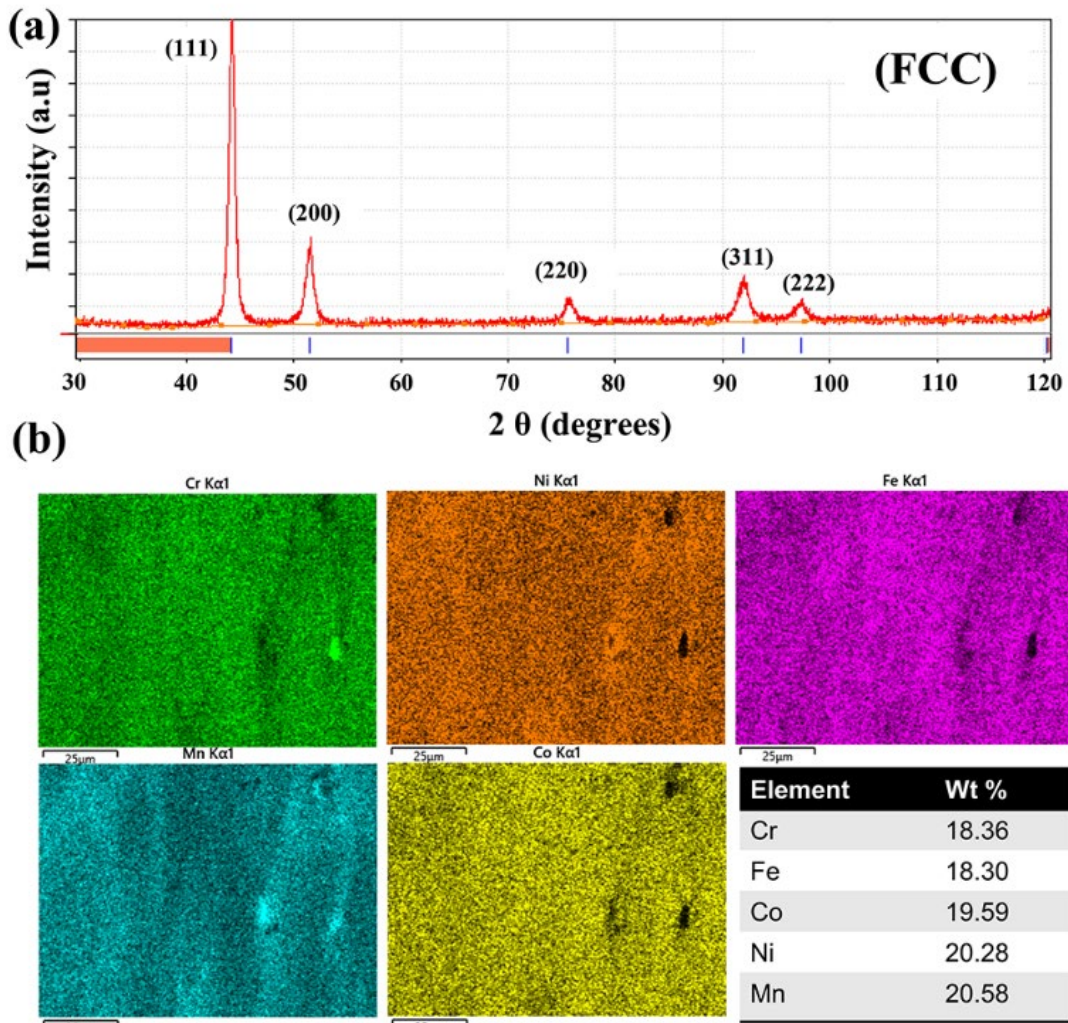


Figure 2: High entropy alloy; XRD phase map (a), EDS maps for individual constituting elements with chemical composition (b)

Figure 3 shows the raw material SEM and EBSD images before deformation. The material consists of almost equiaxed grains with definite grain boundaries. From Figure 3 (a), it can be perceived that the average grain size is larger than 100  $\mu$ m.

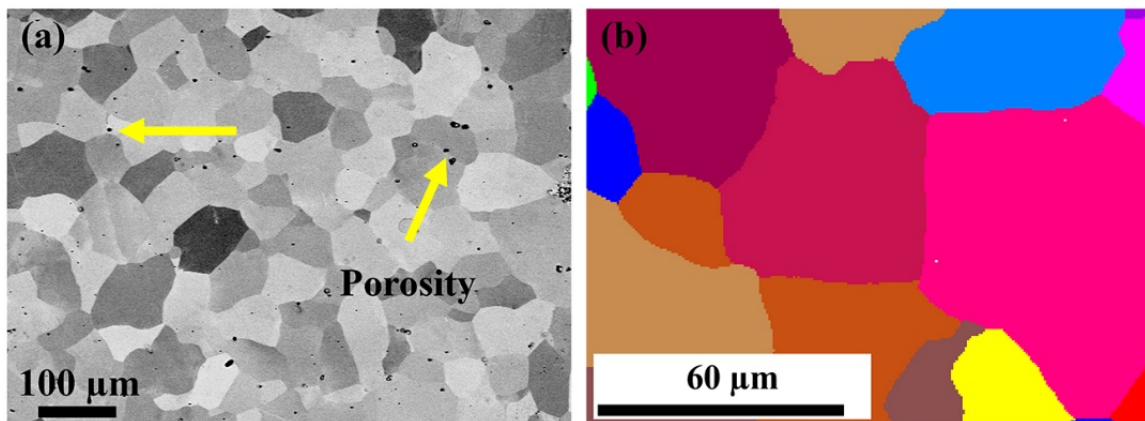


Figure 3: SEM-BSD image (a) and IPF-unique grain color map for raw material



### 3.2 Mechanical characterization

Quasi-static compression was performed at a strain rate of  $10^{-4} \text{ s}^{-1}$  on cubic specimens. Dynamic compression tests at a strain rate of  $1500 \text{ s}^{-1}$  were conducted employing the ESHPB. The acquisition of incident reflected and transmitted signals are made using strain gauges mounted at the center of the bars. The complete operational and construction details of the equipment are available in our previous published work [16]. Tests repeatability was ensured to enhance the validation of results. For dynamic tests, uni-axial stress wave theory can be used to acquire stress, strain, and strain rate from the following relationship;

$$\sigma_s = E \left( \frac{A}{A_s} \right) \epsilon_T \quad (1)$$

$$\epsilon_s = \frac{2C_0}{l_s} \epsilon_R dt \quad (2)$$

$$\dot{\epsilon} = \frac{2C_0}{l_s} \dot{\epsilon}_R \quad (3)$$

In the above equations,  $E$  and  $A$  are the elastic moduli and cross-sectional area of the incident bar,  $C_0$  is the longitudinal wave speed, and  $C_0$  is the longitudinal elastic wave velocity given by  $\sqrt{E/\rho}$ . The  $\epsilon_R$  and  $\epsilon_T$  are the reflected and transmitted wave signals recorded by the strain gauge. From Eq. 1-3, the strain rate during deformation is thus proportional to the reflected pulse amplitude; the stress in

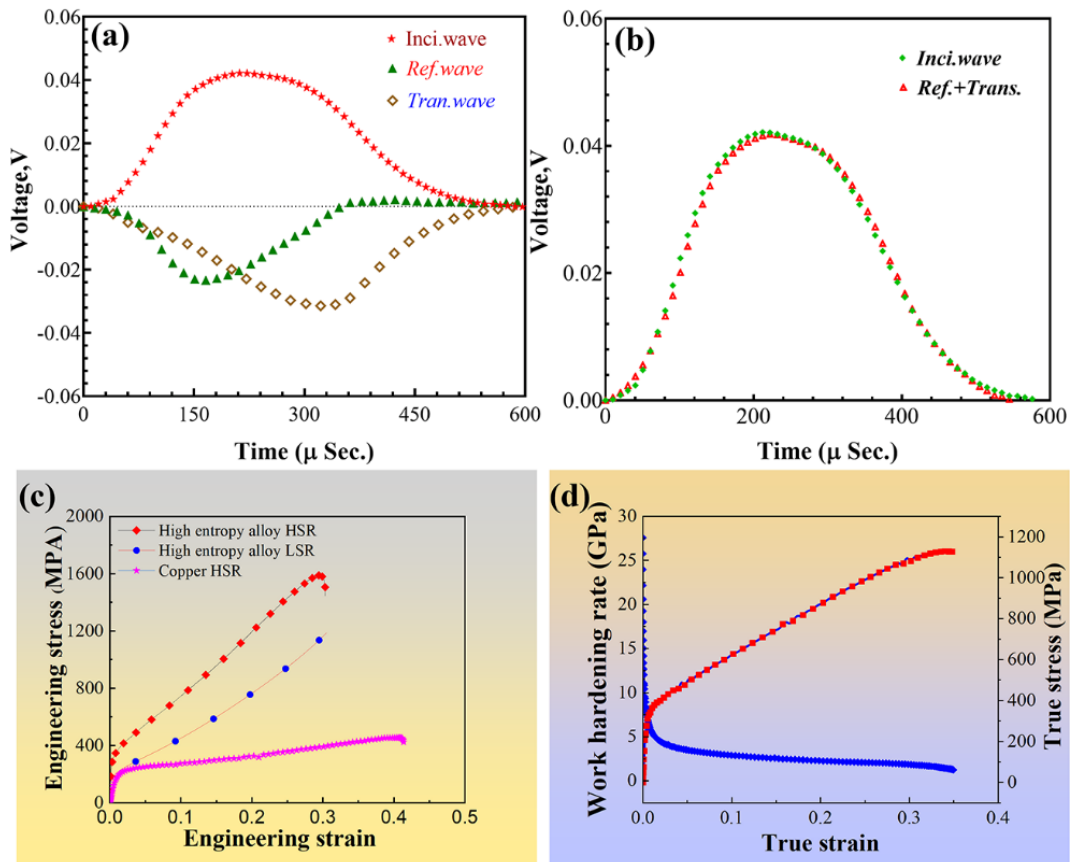


Figure 4: Time history plots for stress wave propagation (a) stress balance curves (b) low and high strain rate compression curves (c) and work hardening curve at high strain rate plotted against true stress

the specimen is proportional to the amplitude of the transmitted pulse, and the axial strain in the specimen can be calculated by integrating the strain rate with respect to time  $t$ . Some salient features of the new novel method adopted in this study for dynamic testing are the constant strain rate and stress balance, attributed to the constant input values of voltage and capacitance as compared to the conventional bar where gas pressure control is always hard to achieve. **Figure 4** (a,b) shows the typical stress pulse generated and related stress balance for the dynamic test carried out in the current study, respectively.

Uniaxial low strain rate tests and high strain rate test results are presented in **Figure 4** (c). The dynamic stress-strain behavior of high entropy alloys has also been compared to pure copper, demonstrating a significant difference in mechanical performance between high entropy alloys and traditional FCC metals and alloys. The engineering stress-strain curves depict salient features of high strain rate dependent strength elevation and profound strain rate sensitivity. The stress-strain curves at the end of the test depict unloading since no fracture of the specimens was observed during the progression of strain. Another prominent feature of the curves suggests bi-linear work-hardening in both the quasi-static and dynamic regimes. With a shift from low to high strain rate, yield strength rises from 189 MPa to 323 MPa, and flow stress jumps from 1043 MPa to 1590 MPa. It can be observed that conventional FCC metals do not manifest such mechanical performance at high strain rates, specifically the excellent work-hardening capability as shown for copper tested at the same high strain rate. Such a uniqueness in the properties proposes this new class of materials as a potential candidate for shock and impact-related applications in future aerospace, automobile, and defense industries, where strengthening of material at high impact loads is vital. The incredible strength elevation with altering scenario of strain rate is attributed to the microstructural changes and the intrinsic atomic-scale arrangements in the high entropy alloys, specifically the lattice distortion and cocktail effect. Unlike simple metals and alloys, due to the equiatomic nature of the elemental distribution, the strain fields produced in high entropy material are explicitly governed by individual elements, which reduce thermal vibrations and increase strength and hardness. Similarly, the cock tail effect, originating from the rule of the mixture and mutual interaction of constitutive elements present in nearly equimolar compositions, imparts excessive properties compared to conventional alloys. The work hardening (WHR) curves for the HEA at a high strain rate are also shown in **Figure 4** (d). It is evident that material has a steady higher WHR than 2000 MPa, which steadily decreases with increasing strain. The curve has two distinctive regions; the first, where the work hardening rate decreases very rapidly, represents the elastic-plastic transition domain. After this, the WHR rate remains almost constant till the end of the strain value is achieved. This region mainly marks the dislocation-glide mediated deformation, and all the surge and elevation in yield strength are governed by dislocation-dislocation interactions, multiplication, and amplification of their density. This feature is discussed in detail in the later section.

### 3.3 Post-compression microstructural evolution

Macroscopically, the specimens after compression were absent of any physical / surface degradation except the volumetric change, which was also absent of any bulging or shearing. These findings show good malleability and compressibility without sacrificing structural integrity. A comprehensive microstructural examination was carried out utilizing EBSD mapping to better comprehend the microscopic changes. Figure 5 (a,c) presents the IPF maps of deformed specimens at LSR and HSR.

Figure 5 (a) that overall the grains approximate the same morphology as raw material (Figure 2), specifically the grain boundary area; however, one salient feature is the variations of color profiles inside individual grains, which become more prominent at higher strain rates. These color gradients are, in fact, related to the deformation and strain rate induced changes and are contributed by the dislocation movements and generation within the grains as the plastic deformation proceeds.

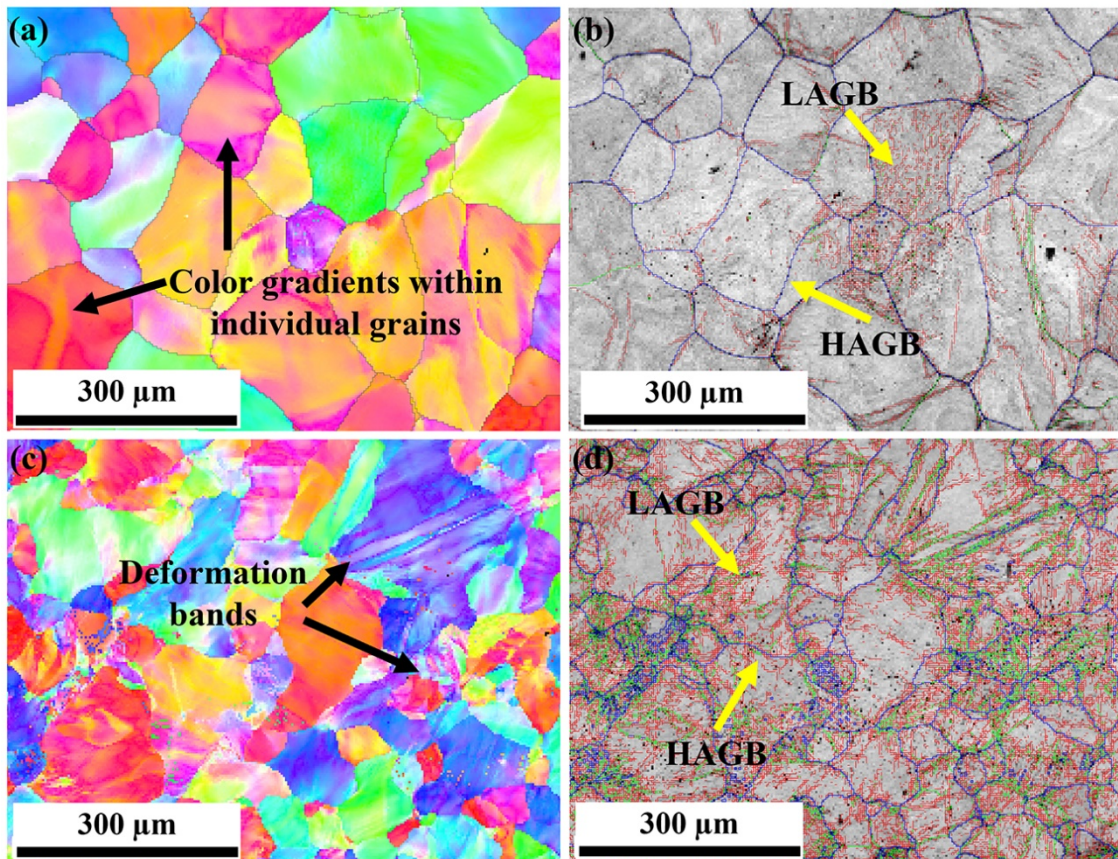


Figure 5: EBSD-IPF and grain boundary maps for LSR (a,b) and HSR (c,d)

It is well established that the impediments that must be overcome during dislocation movement can be categorized into two kinds: a long-range athermal barrier (non-thermally activated) controlled by the material structure and a short-range barrier (thermally activated barrier) that can be influenced by the thermal energy which is governed by thermal fluctuations. However, due to the very short durations involved in HSR loading, the thermal energy effects decrease, and it becomes hard for dislocations to overcome thermal barriers, resulting in elevated flow stress [17]. Another proposed reason for amplified strength during dynamic conditions is the formation of multiple deformation bands and excessive volume of low-angle grain boundaries (LAGB). These two features are explicitly related to the grain misorientation during high strain rate tests and, quantifiably speaking, influence the overall strengthening effect. LAGB can act in two manners; providing new sites for dislocation nucleation or acting as a barrier to either impede the mobility of dislocations or facilitate the selective transfer of dislocations [18] to help deformation proceed. At the same time, the dislocation mobility is suppressed, and the flow stress increases. Besides with progression of deformation, the work hardening also becomes excessively greater due to the lesser time available for recovery and relaxation of dislocation source. This manifestation causes increased dislocation density and hence elevated strengthening, as is observed in the stress-strain behavior of the alloy. The microstructural feature as observed in **Figure 5** (b,d), is akin to the aforesaid phenomena and provides insight into the formation of excessive low angle grain boundaries (misorientation less than  $15^\circ$ ). These LAGB are arrays of dislocations within the grains which form during the deformation of the material. Both quasi-statically and dynamically compressed samples have an enormous quantity of LAGBs as compared to undeformed structures, which consist only of high angle grain boundaries (misorientation greater than  $15^\circ$ ). HSR sample also shows a relatively larger amount of LAGB as compared to a material tested at LSR that is resultant in the strain rate effect (since the deformation level is approximately the same in LSR and HSR tests). The LAGB migration, which is governed by the collective motion of its constituting dislocations, is easier, and it favors the plasticity of material[19].

#### **4. Summary and conclusions**

The investigations carried out on a high entropy alloy at low and high strain rates show that this new class of materials exhibits far better mechanical performance and characteristics as compared to the metal counterparts with the same phase structure. The high strain rate behavior of the material tested under the current study shows that;

- i. The strengthening effect in the material is attributed to the intrinsic unique elemental combination, which results in lattice distortion and cock-tail type effect.
- ii. The high strain rate strength is mainly attributed to the dislocation nucleation amplification.
- iii. The excellent structural integrity at high strain rates provides insight for utilizing the high entropy alloys as promising future structural materials in impact-related scenarios, especially in aerospace and automobile.

#### **Acknowledgments**

This work is sponsored by the National Natural Science Foundation of China ,111 Project (No. BP0719007).



## References

- [1] B. Cantor, I. T. H. Chang, P. Knight, and A. J. B. Vincent, "Microstructural development in equiatomic multicomponent alloys," *Materials Science and Engineering: A*, vol. 375-377, pp. 213-218, 2004.
- [2] J. W. Yeh *et al.*, "Nanostructured high-entropy alloys with multiple principal elements: novel alloy design concepts and outcomes," *Advanced engineering materials*, vol. 6, no. 5, pp. 299-303, 2004.
- [3] J.-W. Yeh, "Recent progress in high-entropy alloys," *Annales de Chimie Science des Matériaux*, vol. 31, no. 6, pp. 633-648, 2006.
- [4] B. Wang *et al.*, "Mechanical Properties and Microstructure of the CoCrFeMnNi High Entropy Alloy Under High Strain Rate Compression," *Journal of Materials Engineering and Performance*, vol. 25, no. 7, pp. 2985-2992, 2016.
- [5] X. Feng *et al.*, "Heavily twinned CoCrNi medium-entropy alloy with superior strength and crack resistance," *Materials Science and Engineering: A*, vol. 788, p. 139591, 2020.
- [6] J.-P. Liu, J.-X. Chen, T.-W. Liu, C. Li, Y. Chen, and L.-H. Dai, "Superior strength-ductility CoCrNi medium-entropy alloy wire," *Scripta Materialia*, vol. 181, pp. 19-24, 2020.
- [7] "<Microstructure and Properties of Al05CoCrCuFeNiTi.pdf>."
- [8] S. Varalakshmi, M. Kamaraj, and B. S. Murty, "Synthesis and characterization of nanocrystalline AlFeTiCrZnCu high entropy solid solution by mechanical alloying," *Journal of Alloys and Compounds*, vol. 460, no. 1-2, pp. 253-257, 2008.
- [9] F. Jiang *et al.*, "In-situ formed heterogeneous grain structure in spark-plasma-sintered CoCrFeMnNi high-entropy alloy overcomes the strength-ductility trade-off," *Materials Science and Engineering: A*, vol. 771, p. 138625, 2020.
- [10] P. Chauhan, S. Yebaji, V. N. Nadakuduru, and T. Shanmugasundaram, "Development of a novel light weight Al35Cr14Mg6Ti35V10 high entropy alloy using mechanical alloying and spark plasma sintering," *Journal of Alloys and Compounds*, vol. 820, p. 153367, 2020.
- [11] D. Yan *et al.*, "Microstructures, Mechanical Properties, and Corrosion Behaviors of Refractory High-Entropy ReTaWNbMo Alloys," *Journal of Materials Engineering and Performance*, vol. 29, no. 1, pp. 399-409, 2020.
- [12] B. Wang, X. Huang, Y. Liu, and B. Liu, "Mechanical Properties and Shear Localization of High Entropy Alloy CoCrFeMnNi Prepared by Powder Metallurgy," pp. 469-480, 2018.
- [13] C. T. Wang *et al.*, "Strain Rate Effects on the Mechanical Properties of an AlCoCrFeNi High-Entropy Alloy," *Metals and Materials International*, vol. 27, no. 7, pp. 2310-2318, 2021.
- [14] S. G. Ma, Z. M. Jiao, J. W. Qiao, H. J. Yang, Y. Zhang, and Z. H. Wang, "Strain rate effects on the dynamic mechanical properties of the AlCrCuFeNi<sub>2</sub> high-entropy alloy," *Materials Science and Engineering: A*, vol. 649, pp. 35-38, 2016.
- [15] H. Nie, T. Suo, X. Shi, H. Liu, Y. Li, and H. Zhao, "Symmetric split Hopkinson compression and tension tests using synchronized electro-magnetic stress pulse generators," *International Journal of Impact Engineering*, vol. 122, pp. 73-82, 2018/12/01/ 2018.
- [16] H. Nie, T. Suo, B. Wu, Y. Li, and H. Zhao, "A versatile split Hopkinson pressure bar using electro-magnetic loading," *International Journal of Impact Engineering*, vol. 116, pp. 94-104, 2018/06/01/ 2018.
- [17] T. Zhang, Z. Jiao, Z. Wang, and J. Qiao, "Dynamic deformation behaviors and constitutive relations of an AlCoCr<sub>1.5</sub>Fe<sub>1.5</sub>NiTi<sub>0.5</sub> high-entropy alloy," *Scripta Materialia*, vol. 136, pp. 15-19, 2017.
- [18] S. Chen and Q. Yu, "The role of low angle grain boundary in deformation of titanium and its size effect," *Scripta Materialia*, vol. 163, pp. 148-151, 2019.
- [19] J. T. M. De Hosson *et al.*, "In situ TEM nanoindentation and dislocation-grain boundary interactions: a tribute to David Brandon," *Journal of Materials Science*, vol. 41, no. 23, pp. 7704-7719, 2006/12/01 2006.